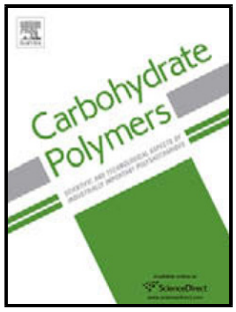

Title: Molecular engineering of manipulated alginate-based polyurethanes

Author: Hamed Daemi Mehdi Barikani

PII: S0144-8617(14)00599-2
DOI: http://dx.doi.org/doi:10.1016/j.carbpol.2014.06.023
Reference: CARP 8988

To appear in:

Received date: 11-3-2014
Revised date: 7-5-2014
Accepted date: 3-6-2014

Please cite this article as: Daemi, H., and Barikani, M.,Molecular engineering of manipulated alginate-based polyurethanes, *Carbohydrate Polymers* (2014), http://dx.doi.org/10.1016/j.carbpol.2014.06.023

Molecular engineering of manipulated alginate-based polyurethanes

*Hamed Daemi, Mehdi Barikani**

Department of Polyurethane and Nanopolymers, Iran Polymer and Petrochemical Institute, P.O. Box 14965/115, Tehran, Islamic Republic of Iran

Abstract

The novel soluble alginate-based polyurethanes in organic solvents were synthesized by the reaction of NCO-terminated prepolymers and tributylammonium alginate (TBA-Alg) for the first time. The chemical structures of synthesized polyurethanes were characterized using FTIR, ^{1}H NMR and TGA. The reaction completion was confirmed by disappearing of NCO band in FTIR spectra. Furthermore, a peak at 4.71 ppm and some small peaks at a range of 4.12–4.37 ppm in the ^{1}H NMR of alginate-based polyurethanes were assigned to the backbone of alginate. The results of both FTIR and ^{1}H NMR were remarkably confirmed by TGA data. The ionic nature of polyurethane backbone not only affects on thermal properties of samples, but it also changes the chemically-bonded alginate morphology. Both polyether and polyester based non-ionic polyurethanes extended by TBA-Alg illustrated the distinct alginate, whereas those ionomers extended by alginate were appeared as the continuous systems at nanoscale.

Keywords

TBA-Alginate, Polyurethane, Organic solvent, Chemical modification, Chemical characterization

1. Introduction

Alginate is a naturally occurring biopolymer with a broad range of unique features for example biodegradability, biocompatibility, non-toxic and non-immunogenic properties (Lee, & Mooney, 2012; Van den Bos, Dinkelaar, Overkleeft, & Van der Marel, 2006; Wong, 2011; Yeo, & Kim, 2014). Alginate is not only used as a biopolymer in biological, medical and drug delivery systems but also in a variety of industrial processes (Gibbs, Kermasha, Alli, & Mulligan, 1999). Today, commercial alginates are extracted from different sources of algae. There are a broad range of diverse alginates with different chemical properties respect to their seasonal and growth conditions (Ghadban, Albertin, Rinaudo, & Heyraud, 2012). The chemical and structural properties of these biopolymers are determined by the sequence of two types of hexuronic acid monomers including α-l-guluronic acid (G) and β-d-mannuronic acid (M) residues. Furthermore, all of the naturally occurring alginates contain three dissimilar blocks including homogenous G and M blocks and heterogeneous MG ones that have been jointed together by 1→4 glycosidic bonds (Daemi, & Barikani, 2012; Pegg, Jones, Athauda, Ozer, & Chalker, 2014).

Chemical modification of alginates has been reported in both aqueous media and organic solvents (Babak et al., 2000; Leone, Torricelli, Chiumiento, Facchini, & Barbucci, 2008; Pawar, & Edgar, 2011; Pelletier, Hubert, Lapicque, Payan, & Dellacherie, 2000). Alginates have four reactive sites for contribution in a chemical reaction including carboxylic acid and hydroxyl functional groups, and two relatively not sustainable bonds, i.e. 1→4 glycosidic and internal glycolic bonds. Some of important characteristics of alginate derivatives for example hydrophilicity, solubility, and chemical and biological properties may be modified by creating new functional groups into the alginate backbone (Pawar, & Edgar, 2012). Esterification, amidation, oxidation, counter ion exchange reaction and some of miscellaneous reactions are the most important chemical procedures to modify alginate (Yang, Xie, & He, 2011). The hydrophobic nature of neat alginate is modified through the functionalization of the carboxylic acid groups. Hydroxyl functional groups are usually modified by a simple coupling reaction, sulfation or copolymerization. Finally, glycosidic and internal glycolic bonds can be chemically treated by acidic or alkaline aqueous solutions and oxidation reactions, respectively (Ghadban, Reynaud, Rinaudo, & Albertin, 2013; Ruvinov, Leor, & Cohen, 2011).

Polyurethanes (PUs), a category of highly significant engineering polymers, are introduced by their excellent properties and a broad range of applications (Chattopadhyay, & Webster, 2009; Tang et al., 2013). The urethane chemical bonds are synthesized through a polyaddition reaction between an isocyanate and a hydroxyl functional

group (Daemi, RezaieyehRad, Barikani, & Adib, 2013). It is possible to obtain a special grade of polyurethane by changing the block ratio, the types of isocyanate and hydroxyl-containing compounds, the selection of an amine or a hydroxyl chain extender, the type of reaction and so on (Barikani, Zia, Bhatti, Zuber, & Bhatti, 2008; Lligadas, Ronda, Galià, & Cádiz, 2007; Madbouly, Otaigbe, Nanda, & Wicks, 2005). Polyurethanes have a biphasic microstructure including soft segments and hard domains. The amount of phase separation between these segments determines the final properties of the polyurethane sample (Oniki et al., 2013).

The synthesis of carbohydrate based polyurethanes or blending of those aqueous solutions with PUDs for example chitin, chitosan, cellulose and starch for attaining the biocompatible and miscible binary polymeric systems have been studied during recent years (Kim, Kwon, Yang, & Park, 2007; Pei, Malho, Ruokolainen, Zhou, & Berglund, 2011; Saralegi et al., 2013; Shih, & Huang, 2003; Zia, Anjum, Zuber, Mujahid, & Jamil, 2014). Through the well-known carbohydrate based polyurethanes, preparation of those alginate-based had been a significant challenge because of the final polymer's tendency to the phase separation (Travinskaya, & Savelyev, 2006). Recently, we introduced some interesting procedures including the using excess diisocyanate compared to the block ratio, the blending of SA with a new generation of PUDs and dispersing the alginate nanoparticles on the cationic polyurethane matrix to overcome the obvious incompatibility of mentioned polymers (Daemi, Barikani & Barmar; 2014; Daemi, Barikani & Barmar; 2013; Daemi, Barikani & Barmar, 2013). Nevertheless, the preparation of compatible alginate-based polyurethanes with desired properties is an open challenge. Here, we describe the synthesis and characterization of the novel soluble alginate-based polyurethanes in common aprotic organic solvents for the first time.

2. Experimental

2.1. Chemicals

Polytetramethylene ether glycol (PTMEG) with a molecular weight 950−1000 was obtained from Arak Petrochemical Company. Polypropylene glycol (PPG) and polycaprolactone diol (PCL) with molecular weight 2,000 were supplied by Merck and Solvay, respectively. The mentioned polyols were dried at 60 °C under vacuum for 12 h before use to ensure the removal of all moisture that may interfere with the isocyanate reactions. Dimethylol propionic acid (DMPA) (Aldrich) was dried at 100 °C and used without purification. Tributylamine (TBA), dimethyl sulfoxide (DMSO), N,N−dimethylformamide (DMF) and N-methylpyrrolidone (NMP) were purchased from Merck, Germany and dried using 4 Å molecular sieves. In addition, both isophorone diisocyanate

(IPDI) and toluene diisocyanate (TDI) were obtained from Merck. Sodium alginate (SA) with a molecular weight 12,000–40,000 was purchased from Aldrich and used as received.

2.2. Synthesis of TBA-Alginate

Alginic acid was synthesized through a procedure described by Babak et al., (2000) with some modifications. Sodium alginate (4 g) was added to a mixture of HCl (0.6 N, 50 mL) and ethanol (40 mL) and stirred overnight at 4 °C. The solid fracture, alginic acid, was separated by filtration under vacuum using a coarse filter paper. Then, the alginic acid was purified by washing with ethanol and acetone and dried in the oven at 60 °C. In the next step, dried alginic acid was dispersed in 50 mL of water and neutralized (pH=7.0) by tributylamine under controlled-delivery conditions to obtain the TBA-alginate, a soluble form of alginate in polar aprotic organic solvents.

2.3. Synthesis of DMPA extended PU ionomer

The neat polyurethane ionomer was prepared as reported previously (Daemi, Barikani, & Barmar, 2013). In brief, proper amounts of IPDI and PTMEG were reacted in a 100-cm^3 round-bottomed, three-necked flask equipped with a magnetic stirrer, heating oil bath, condenser, thermometer and the N_2 purge system to obtain the NCO-terminated prepolymer. After 3 h, a solution of DMPA in NMP was added into the reactor and stirring continued for 1 h. Finally, the carboxylic acid groups of DMPA were neutralized by addition of TEA to the mixture and a polyurethane ionomer was obtained (PU 1).

2.4. Synthesis of TBA-Alg extended PU ionomer

For probing of TBA-Alg impact on the chemical structure of polyurethane, a similar anionic PU ionomer extended by modified alginate was synthesized (Scheme 1). The catalyst-free synthesis of TBA-Alg extended PU (PU 2) was performed through the polyaddition reaction of modified alginate with urethane prepolymer. Initially, the IPDI and PTMEG were mixed to obtain a NCO-terminated prepolymer. Afterward, the chain extension of prepolymer was initiated by DMPA and continued with the TBA-Alg solution. The reaction of diol chain extenders by free isocyanate functional groups was completed at 30 min and 6 h, respectively. The synthesized polyurethane was casted onto the Teflon plate and cured in oven at 100 °C for 12 h. The compositions of alginate-based polyurethanes are listed in Table 1.

2.5. Synthesis of TBA-Alg extended PPG-based polyurethanes

The NCO-terminated prepolymer was synthesized by the reaction of TDI and PPG in a 100-cm^3 round-bottomed, three-necked flask. For this aim, TDI was added dropwise to the PPG at 60 °C for 2 h under nitrogen atmosphere

until the theoretical NCO content was reached. Then, proper amount of TBA-Alg in DMSO was added into the reactor at 90 °C and the reaction was completed after 6 h (PU 4) (Scheme 2). For film formation, the solution of polyurethane was casted onto the plate and dried at 100 °C for 12 h.

2.6. Measurements

The IR spectra of synthesized polyurethanes were performed with a Bruker-Equinox 55 FTIR spectrometer (Ettlingen, Germany) which equipped by ATR accessories with a ZnSe crystal. The ^{1}H NMR spectra were recorded in deuterated dimethyl sulfoxide (DMSO)-d_6 solution using a Bruker DRX-250 Avance spectrometer (Germany). The chemical shifts (δ) were reported in ppm by using tetramethylsilane (TMS) as a standard. Thermogravimetric analysis (TGA) was recorded on a Polymer Lab TGA-1500 instrument (London) under a nitrogen atmosphere from 25 °C to 600 °C with a heating rate of 10 °C/min. Scanning Electron Microscopy (SEM) (Model Vega, Tescan Co., Czech Republic) was served to probe the morphological aspects of TBA-Alg extended polyurethane. Characterization of synthesized PUs in a microscale was performed using EDX method (Oxford instrument, model INCA).

3. Results and discussion

3.1. Molecular characterization

Initially, we examined the solubility of TBA-Alg in three common polar aprotic organic solvents, i.e. DMSO, DMF and NMP. The alginate solubility depends on different parameters for example the number of carboxylic acid groups in the backbone, the presence of bulky carbon structures, the chemical modification type of alginate bulk, the counter ion of carboxylate groups in the backbone, the polarity of solvent to overcome the hydrogen bonding present in the polymer and the nature of heteroatom in chemical structure of organic solvent (Valle, & Romeo, 1995).

The chemical modification of alginates by alkylammonium salts is a common procedure to obtain soluble modified alginate in polar organic solvents. Tetrabutylammonium and tributylammonium salts are the most common alkylammonium precursors for chemical modification of alginate bulk. In this regard, Pawar et al. (2011) have reported that an auxiliary such as tetrabutylammonium fluoride trihydrate can promote the alginate solubility in organic solvents. Both the using tetrabutylammonium hydroxide via an ion-exchange resin and direct hydrophobization by tributylammonium salt are the most common procedures for attaining soluble alginate (Guo, & Conrad, 2002; Song, Chen, Yu, Linliu, & Tseng, 1996).

For obtaining a solution of TBA-Alg in organic solvents, 0.1 g of TBA-Alg was dissolved in 10 mL of mentioned solvents and a clear solution was obtained by heating at 50 °C after 2 h. Furthermore, the ultimate accessible concentration of soluble modified alginate was 3% w/w in organic solvents. The solution of tetrabutylammonium alginate in DMF with concentration 2.5% w/w is the maximum solubility of modified alginate which has been reported so far however, we obtain the solutions with 3% w/w for the first time. Based on the observations, the synthesized TBA-Alg was completely soluble at a concentration of 10 mg/mL in all mentioned single-component polar aprotic solvents.

All polyurethane systems were synthesized via the step-growth reaction of polyether diol or polyester diol and a diisocyanate. The final alginate-based polyurethanes were synthesized by the addition of the solution of TBA-Alg in DMF or DMSO under catalyst-free conditions because the samples were prepared for subsequently biological tests. The compositions of all synthesized polyurethane samples are listed in Table 1. We found that either Alg-based PU ionomers or those non-ionic are soluble in DMSO and DMF for the concentrations lower than 5% w/w at temperatures more than 80 °C. The chemical structure of synthesized polyurethanes extended by modified alginate was characterized by FTIR and ^{1}H NMR spectroscopic techniques.

3.2. FTIR Analysis

The Fourier transform infrared (FTIR) spectra of the sodium alginate, neat polyurethane, and the polyurethanes extended by modified alginate are shown in Fig. 1. Chemical structure of sodium alginate was confirmed by appearance of three absorption bands including stretching vibrations of O–H bonds, and both asymmetric and symmetric stretching vibrations of carboxylate groups at 3393, 1649 and 1460 cm^{-1}. Furthermore, the stretching vibrations of C–O bonds were appeared at 1107 cm^{-1}.

The chemical structure of neat polyurethane ionomer (PU 1) was characterized by appearance the stretching vibrations of the N–H, C=O and amide II bands at 3322, 1713 and 1537 cm^{-1}, respectively. The observed bands at the range of 1000–1150 cm^{-1} were assigned to the C–O–C stretching vibrations of the soft segment.

FTIR spectrum of anionic polyurethane extended by TBA-Alg is performed to verify the disappearance of the NCO band at 2270 cm^{-1}. The appearance of stretching vibrations of the N–H at 3387 cm^{-1}, C=O at 1719 $cm^{-1}$and N–H for amide II at 1561 cm^{-1} also confirmed the polyurethane structure. The stretching and bending vibrations of alkyl groups were appeared at 2796–2950 cm^{-1} and 1310–1465 cm^{-1}, respectively. Moreover, two novel absorption bands were appeared at 1638 $cm^{-1}$and 819 cm^{-1} for both ionic and non-ionic alginate-based polyurethanes. These

new bands were ascribed to the asymmetric stretching vibrations of carboxylate groups and uronic acid residues of alginate, respectively. Therefore, the alginate insertion into the polyurethane backbone can be clearly confirmed by FTIR results. Finally, the proposed chemical structure of synthesized TBA-Alg extended PPG-based PU was approved by the creation of carbonyl groups of urethane at 1740 cm^{-1}.

3.3. ^{1}H NMR Spectroscopy

^{1}H NMR spectra of both neat and alginate-based polyurethane ionomers are shown in Fig. 2. The alginate-free polyurethane was characterized by appearance of the weak peaks of cis and trans conformers of urethane N–H groups at 6.88–7.09 ppm, respectively (Fig. 2a). Furthermore, the protons of urethane CH_2 groups of PTMEG and DMPA were observed at 3.86 and 3.97 ppm, respectively. The methyl protons of IPDI were appeared at 0.82–0.93 ppm. The observed peaks at 0.93–1.04 ppm were assigned to the methyl group of DMPA and some methylene groups of IPDI. The methylene groups of soft segment and the ethyl groups of tertiary ammonium were observed at 1.42–1.47 ppm. Finally, the appeared sharp peak at 3.27 ppm was attributed to the CH_2–O protons of repeating units of PTMEG.

The ^{1}H NMR spectrum of alginate-based polyurethane is shown in Fig. 2b. A broad peak at 4.71 ppm and some small peaks at a range of 4.13–4.37 ppm are the most important new peaks in the spectrum of polyurethane extended by modified alginate. The observed peak at 4.71 ppm was ascribed to anomeric protons of modified alginate. Furthermore, the several appeared peaks at 4.12–4.37 ppm were ascribed to the backbone of alginate for example, the protons of mannuronate and guluronate residues. Both latter peaks confirmed the incorporation of modified alginate in the backbone of polyurethane. The urethane N–H groups and the protons close to the urethane functional groups were observed at 6.93–7.20 ppm and 3.92–4.00 ppm, respectively. The lower chemical shifts were assigned to the other aliphatic protons of IPDI, alginate backbone, butyl chains of tertiary ammonium and PTMEG segments.

Fig. 2c shows the spectrum of neat sodium alginate in D_2O as the solvent. NMR spectroscopy has proven to be an expeditious characterization technique for alginates. The signals of the anomeric protons, i.e. G-1, GM-5, M-1 and GG-5 protons, were appeared at a range of 4.40–4.90 ppm. The observed signals at 3.83–4.03 and 3.61–3.76 ppm were assigned to the residual protons of G monomer including G-2, G-3, G-4 and other protons of M residues, respectively. The comparison of the ^{1}H NMR spectrum of sodium alginate with synthesized polyurethane samples supported the proposed structures.

The ^{1}H NMR spectrum of nonionic PPG-based polyurethane extended by TBA-Alg is shown in Fig. 3. The crowded region at 6.80−8.14 ppm was assigned to the protons of aromatic ring and the urethane groups. The C–H protons of PPG and the anomeric protons of alginate were observed at 4.84 and 4.02−4.38 ppm, respectively. Eventually, the aliphatic protons of PPG and the other protons of alginate backbone were appeared at lower chemical shifts.

3.4. TG Analysis

The insertion of TBA-Alg into the PU backbone was also confirmed by TGA data (Table 2). It has been reported that the more easily formed urethanes are less stable (Chattopadhyay, & Webster, 2009). For instance, the urethane functional groups that are formed by an aliphatic isocyanate and an alkyl alcohol have a higher degradation temperature than other systems (Petrovic, Zavargo, Flynn, & Macknight, 1994). As the first result, the degradation temperatures of TDI and IPDI based PUs extended by TBA-Alg were appeared at 200 °C and 250 °C, respectively (Fig. 3). The low-temperature degradation of TDI–PPG based PU has an appropriate correlation with observations of Ingham et al. (1964). Moreover, the observed weight loss at temperatures above 250 °C was assigned to the scission of the polyether bonds. The TGA experiments of the synthesized PU showed that IPDI based PUs extended by alginate were more stable than the aromatic diisocyanate (TDI) containing PU at moderate temperatures, while at higher temperature the stability order followed the reverse trend (Chattopadhyay, Sreedhar, & Raju, 2005). The lower thermal resistance of TDI based PU was related to the asymmetrical rigid chains and difficult hard segment–hard segment interactions of PUs (Stanciu et al., 1999).

The PPG-based PU extended by TBA-Alg (PU 4) illustrated an entirely different behavior compared to the alginate-based polyurethane ionomer (PU 2). The second degradation step of PPG-based PU extended by TBA-Alg at 300−350 °C was assigned to the biopolymer degradation. This separated step was not observed for PTMEG-based PU extended by TBA-Alg. It may be ascribed to the dissimilar interactions of modified polar TBA-alginate with asymmetrical chains of PPG-based PU and also the affinity of alginate for agglomeration. The TBA-Alg has been comprised of the extensive ionic groups, therefore these polar groups have an extreme affinity to analogous polar groups. Because of the presence of carboxylate groups in the structure of PU ionomer (PU 2), there is a significant electrostatic interaction between chemically reacted of modified alginate and PU ionomer therefore, the second step was changed to a continuous form. The TBA-Alg chains have chemical bonds by polyurethane backbone, however those have a tendency for agglomeration and show a separated thermal

degradation behavior. The tendency of chemically bonded alginate for agglomeration was also confirmed by SEM images.

3.5. SEM and EDX Analysis

The SEM images of synthesized polyurethanes containing TBA-alginate revealed a novel aspect of alginate morphology through the carbohydrate based PUs. We found the type of polyol and chain extenders have a significant role on the surface morphology of samples. Both images of PPG-based and PTMEG-based polyurethanes extended by TBA-Alg have an appropriate conformity with TGA results. The covalently bonded TBA-Alg to the PPG-based PU (PU 4) showed a uniform pattern, including separated white domains through the PU surface (Figs. 4a-c). As was discussed, PPG-based polyurethanes extended by TBA-Alg shows a two-step thermal degradation because of phase separation of modified alginates from PU backbone. It is possible to suppose that TBA-Alg starts to the separate from PU chains due to the non-polar nature of soft segment. Therefore, the modified alginates interact electrostatically each other and create aggregate-like structures.

On the other hand, PTMEG-based polyurethanes extended by TBA-Alg (PU 2) illustrated a continuous morphology, even on nanoscale. This observation may be ascribed to the highly dominant ionic interactions between ammonium groups of TBA-Alg and carboxylate functional groups of polyurethane. Figs. 4d-4f show that the continuousness of phase homogeneity is repeated among the surface of PTMEG-based polyurethanes extended by TBA-Alg for all scales, from micrometers to nanometers. Some of interesting images that both microparticle and nanoparticles of alginate appeared in the vicinity of each other are shown in Figs. 4g-4i. The one-step thermal degradation of non-ionic alginate-based polyurethanes can be assigned to the foregoing affinity of modified alginate to the ionic centers of PU.

To confirm our idea about the effect of PU chemical structure on alginate morphology, we synthesized a polyester-based PU extended by TBA-Alg and probed its surface morphology. This sample illustrated generally similar morphology compared to PPG-based polyurethanes (Fig. 5). However, the modified alginate was appeared as fully separated nanoparticles in PCL-based PU because of more polar ester functional groups of PCL diols than PPG and the more affinity of chemically bonded TBA-Alg particles to interact with ester groups of PCL through hydrogen bonding. Recently, we have reported the formation of physically bonded nanoalginate particles in the matrix of polyurethane ionomers (Daemi, Barikani, & Barmar, 2013). However, the formation of chemically

bonded nanoalginate in the backbone of non-ionic polyurethane structures is an amazing phenomenon and has not been reported so far.

EDX analysis was served for investigation of nitrogen atom's distribution in PTMEG-based polyurethanes extended by TBA-Alg (PU 2), i.e. urethane moieties of polymer backbone and ammonium groups of TBA-Alg, for both an area of sample image without alginate, which was really a challenge, and alginate aggregates. The challenge of finding an area which was empty of alginate had arisen from tremendous continuity between TBA-Alg and the backbone of polyurethane ionomer. As seen in Fig. 6, the nitrogen mapping is approximately uniform for all parts of both polyurethane matrix and polyurethanes containing modified alginate. The nitrogen mapping of polyurethane, i.e. the area which was empty of alginate, was simply assigned to the urethane bonds, while the ammonium groups of modified alginate also participated in mapping of the fractions containing TBA-Alg.

4. Conclusion

The insertion of chemically bonded alginate into the polyurethane backbones was performed by step growth of the NCO-terminated prepolymer and an organic solution of modified alginate, i.e. tributylammonium alginate. The FTIR spectra of synthesized TBA-Alg extended polyurethanes were distinctive compared to those alginate-free by appearance of two new asymmetric stretching vibrations of carboxylate groups and uronic acid residues of alginate. Furthermore, the specific peaks of uronic acid residues in ^{1}H NMR revealed the presence of TBA-Alg into the backbone of polyurethane. TGA observations showed that the nature of polyol and the ionic functional groups of polyurethane backbones have significant impacts on thermal properties of samples. Finally, the morphology of TBA-Alg extended PU ionomer was distinct from those non-ionic analogous. The polyurethane ionomers extended by alginate illustrated a continuous morphology even at nanoscale, while those non-ionic samples were known by aggregate-like structures of alginate into the matrix of polyurethane.

References

Babak, V. G. Skotnikova, E. A. Lukina, I. G. Pelletier, S. Hubert, P. & Dellacherie, E. (2000). Hydrophobically associating alginate derivatives: surface tension properties of their mixed aqueous solutions with oppositely charged surfactants. *Journal of Colloid and Interface Science*, *225*, 505–510.

Barikani, M. Zia, K. M. Bhatti, I. A. Zuber, M. and Bhatti, H. N. (2008). Molecular engineering and properties of chitin based shape memory polyurethanes. *Carbohydrate Polymers*, *74*, 621–626.

Chattopadhyay, D. K. Sreedhar, B. & Raju, K. V. S. N. (2005). Influence of varying hard segments on the properties of chemically crosslinked moisture-cured polyurethane-urea. *Journal of Polymer Science Part B: Polymer Physics*, *44*, 102–118.

Chattopadhyay, D. K. & Webster, D. C. (2009). Thermal stability and flame retardancy of polyurethanes. *Progress in Polymer Science*, *34*, 1068–1133.

Daemi, H. & Barikani, M. (2012). Synthesis and characterization of calcium alginate nanoparticles, sodium homopolymannuronate salt and its calcium nanoparticles. *Scientia Iranica*, *19*, 2023–2028.

Daemi, H. RezaieyehRad, R. Barikani, M. Adib, M. (2013). Catalytic activity of aqueous cationic polyurethane dispersions: A novel feature of polyurethanes. *Applied Catalysis A: General*, *468*, 10–17.

Daemi, H. Barikani, M. & Barmar, M. (2013). Highly stretchable nanoalginate-based polyurethane elastomers. *Carbohydrate Polymers*, *95*, 630–636.

Daemi, H. Barikani, M. & Barmar, M. (2013). Compatible compositions based on aqueous polyurethane dispersions and sodium alginate. *Carbohydrate Polymers*, *92*, 490–496.

Daemi, H. Barikani, M. & Barmar, M. (2014). A simple approach for morphology tailoring of alginate particles by manipulation ionic nature of polyurethanes. *International Journal of Biological Macromolecules,* DOI: 10.1016/j.ijbiomac.2014.02.029.

Ghadban, A. Albertin, L. Rinaudo, M. & Heyraud, A. (2012). Biohybrid glycopolymer capable of ionotropic gelation. *Biomacromolecules*, *13*, 3108–3119.

Ghadban, A. Reynaud, E. Rinaudo, M. & Albertin, L. (2013). RAFT copolymerization of alginate-derived macromonomers–synthesis of a well-defined poly(HEMAm)-graft-(1→4)-α-L-guluronan copolymer capable of ionotropic gelation. *Polymer Chemistry*, *4*, 4578–4583.

Gibbs, B. F. Kermasha, S. Alli, I. & Mulligan, C. N. (1999). Encapsulation in the food industry: a review. *International Journal of Food Sciences and Nutrition*, *50*, 213–224.

Guo, S. Y. C. & Conrad, E. H. (2002). Process for the sulfation of uronic acid-containing polysaccharides. *U.S. Pat. 6,388,060*.

Ingham, J. D. & Rapp, N. S. J. (1964). Polymer degradation. II. Mechanism of thermal degradation of polyoxypropylene glycol–toluene 2,4-diisocyanate polymer (POPG–TDI) and a block polyether glycol–TDI polymer. *Journal of Polymer Science Part A*, *2*, 4941–4964.

Kim, D. H. Kwon, O. J. Yang, S. R. & Park, J. S. (2007). Preparation of starch-based polyurethane films and their mechanical properties. *Fibers and Polymers*, *8*, 249–256.

Lee, K. Y. & Mooney, D. J. (2012). Alginate: properties and biomedical applications. *Progress in Polymer Science*, *37*, 106–126.

Leone, G. Torricelli, P. Chiumiento, A. Facchini A. & Barbucci, R. (2008). Amidic alginate hydrogel for nucleus pulposus replacement. *Journal of Biomedical Materials Research Part A*, *84*, 391–401.

Lligadas, G. Ronda, J. C. Galià, M. & Cádiz, V. (2007), Poly(ether urethane) networks from renewable resources as candidate biomaterials: synthesis and characterization. *Biomacromolecules*, *8*, 686–692.

Madbouly, S.A. Otaigbe, J. U. Nanda, A. K. & Wicks, D. A. (2005). Rheological behavior of aqueous polyurethane dispersions: effects of solid content, degree of nutralization, chain extension, and temperature. *Macromolecules*, *38*, 4014–4023.

Oniki, Y. Suzuki, K. Higaki, Y. Ishige, R. Ohta, N. & Takahara, A. (2013). Molecular design of environmentally benign segmented polyurethane(urea)s: effect of the hard segment component on the molecular aggregation states and biodegradation behavior. *Polymer Chemistry*, *4*, 3735–3743.

Pawar, S. N. & Edgar, K. J. (2011). Chemical modification of alginates in organic solvent systems. *Biomacromolecules*, *12*, 4095–4103.

Pawar, S. N. & Edgar, K. J. (2012). Alginate derivatization: a review of chemistry, properties and applications. *Biomaterials*, *33*, 3279–3305.

Pegg, C. E. Jones, G. H. Athauda, T. J. Ozer, R. R. & Chalker, J. M. (2014). Facile preparation of ammonium alginate-derived nanofibers carrying diverse therapeutic cargo. *Chemical Communications*, *50*, 156–158.

Pei, A. Malho, J. M. Ruokolainen, J. Zhou, Q. & Berglund, L. A. (2011). Strong nanocomposite reinforcement effects in polyurethane elastomer with low volume fraction of cellulose nanocrystals. *Macromolecules*, *44*, 4422–4427.

Pelletier, S. Hubert, P. Lapicque, F. Payan, E. & Dellacherie, E. (2000). Amphiphilic derivatives of sodium alginate and hyaluronate: synthesis and physico-chemical properties of aqueous dilute solutions. *Carbohydrate Polymers*, *43*, 343–349.

Petrovic, Z. S. Zavargo, Z. Flynn, J. H. & Macknight. W. J. (1994). Thermal degradation of segmented polyurethanes. *Journal of Applied Polymer Science*, *51*, 1087–1095.

Ruvinov, E. Leor, J. & Cohen, S. (2011). The promotion of myocardial repair by the sequential delivery of IGF-1 and HGF from an injectable alginate biomaterial in a model of acute myocardial infarction. *Biomaterials*, *32*, 565–578.

Saralegi, A. Fernandes, S. C. M. Alonso-Varona, A. Palomares, T. E. Foster, J. Weder, C. Eceiza, A. & Corcuera, M. A. (2013). Shape-memory bionanocomposites based on chitin nanocrystals and thermoplastic polyurethane with a highly crystalline soft segment. *Biomacromolecules*, *14*, 4475–4482.

Shih, C. Y. & Huang, K. S. (2003). Synthesis of a polyurethane–chitosan blended polymer and a compound process for shrink-proof and antimicrobial woolen fabrics. *Journal of Applied Polymer Science*, *88*, 2356–2363.

Song, Y. M. Chen, W. C. Yu, T. L. Linliu, K. & Tseng, Y. H. (1996). Effect of isocyanates on the crystallinity and thermal stability of polyurethanes. *Journal of Applied Polymer Science*, *62*, 827–834.

Stanciu, A. Bulacovschi, V. Condratov, V. Fadei,C. Stoleriu, A. and Balint, S. (1999). Thermal stability and the tensile properties of some segmented poly(ester-siloxane)urethanes. *Polymer Degradation and Stability*, *64*, 259–265.

Tang, Z. Liu, X. Luan, Y. Liu, W. Wu, Z. Li, D. & Chen, H. (2013). Regulation of fibrinolytic protein adsorption on polyurethane surfaces by modification with lysine-containing copolymers. *Polymer Chemistry*, *4*, 5597–5602.

Valle, F. D. & Romeo, A. (1995). New esters of alginic acid. *U.S. Pat. 5,416,205*.

Travinskaya, T. V. & Savelyev, Y. V. (2006). Aqueous polyurethane–alginate compositions: Peculiarities of behavior and performance. *European Polymer Journal*, *42*, 388–394.

Van den Bos, L. J. Dinkelaar, J. Overkleeft, H. S. & Van der Marel, G. A. (2006). Stereocontrolled synthesis of β-d-mannuronic acid esters: synthesis of an alginate trisaccharide. *Journal of the American Chemical Society*, 128, 13066−13067.

Wong, T. W. (2011). Alginate graft copolymers and alginate-co-excipient physical mixture in oral drug delivery. *Journal of Pharmacy and Pharmacology*, *63*, 1497−1512.

Yang, J. S. Xie, Y. J. & He, W. (2011). Research progress on chemical modification of alginate: A review. *Carbohydrate Polymers*, *84*, 33−39.

Yeo, M. G., & Kim, G. H. (2014). Cell-printed hierarchical scaffolds consisting of micro-sized polycaprolactone (PCL) and electrospun PCL nanofibers/cell-laden alginate struts for tissue regeneration. *Journal of Materials Chemistry B*, 2, 314−324.

Zia, K. M. Anjum, S. Zuber, M. Mujahid, M. & Jamil T. (2014). Synthesis and molecular characterization of chitosan based polyurethane elastomers using aromatic diisocyanate. *International Journal of Biological Macromolecules,* DOI:10.1016/j.ijbiomac.2014.01.073.

355 **Scheme Captions**

356 Scheme 1. Chemical procedure for synthesis of TBA-Alg extended PU ionomer.

357 Scheme 2. Chemical procedure for synthesis of TBA-Alg extended PPG-based PU.

358

Figure Captions

Fig. 1. FTIR spectra of sodium alginate, neat PU ionomer (PU 1), TBA-Alg extended PU ionomer (PU 2) and TBA-Alg extended PPG-based (PU 4).

Fig. 2. ^{1}H NMR spectra of (a) neat polyurethane extended by DMPA, (b) TBA-Alg extended PU ionomer, (c) sodium alginate and (d) PPG-based PU extended by TBA-Alg.

Fig. 3. TGA data of SA and synthesized polyurethanes

Fig. 4. Morphology of TBA-Alg extended PU ionomer (PU 2): (a) milli-sized particles of brittle alginate-based PU ionomers, (b) homogenous morphology of chemically bonded alginate into the polyurethane backbone, (c) significant nanoscale continuity between alginate and PU backbone, (d) alginate's tendency to microscale phase separation from non-ionic backbone, (e) and (f) alginate agglomerates on the matrix of polyurethane, (g) to (i) the alginate microparticles and nanoparticles in the vicinity of each other.

Fig. 5. Significant microscale phase separation of alginate from the matrix of PCL-based non-ionic polyurethane (a) at microscale, and (b) nanoscale.

Fig. 6. The nitrogen mapping: (a), (b) an approximately alginate-free area, and (c), (d) TBA-Alg extended PU ionomer.

373 **Tables**

- Bimodal and monomodal dextran surfactant polymers were synthesized.
- SPR chips were prepared via mixed physisorption of the surfactant polymers.
- A model of the mixed surfactant matrix layer was proposed based on the AFM images.
- Separation distances between the molecules on the chip could be tuned.
- Yellow head viruses could be detected via SPR using the mixed surfactant chips.

Table 1

	Bimodal surfactants		**Monomodal surfactant**
	4dex$_{10k+1.5k}$-surf	**13**dex$_{10k}$-surf	dex$_{1.5k}$-surf
Feed compositions (mol%)[a]			
carboxylic dextran 10K	8	30	0
dextran 1.5K	100	100	100
Compositions measured by ^{1}H-NMR (mol%)[b]			
carboxylic dextran 10K	4.4	11.5	0
C/N ratio of some intermediate products			
PVAm	2.48	2.48	2.48
PVAm-*g*-dextran 1.5k	-	-	15.51
PVAm-*g*-dextran 10K	16.87	48.52	-
PVAm-*g*-allyl dextran 10K	16.78	48.78	-
PVAm-*g*-ally dextran 10K /dextran 1.5K	28.67	48.23	-
Compositions estimated from C/N ratios (mol%)			
carboxylic dextran 10K	3.9	12.6	0
dextran 1.5K	22.0	0	24.1
Estimated number of groups per surfactant molecule[c]			
carboxylic dextran 10K	92	300	0
dextran 1.5K	522	0	572
Grafting distance between carboxylic dextran 10K (d, nm)[d]	6.5	2.0	n/a
Roughly estimated dimensions of a molecular aggregate[e]			
occupied volume (nm^3)	24,000	52,000	2,060
lateral cross-section (nm)	60	75	25

[a] Calculated based on vinyl amine units. [b] Estimated as the a/n value, where a = (integral of peak c′)/62 (i.e., 62 protons from H1 of the dextran backbone) and n = {(integral of peak a) – 3a}/5 (i.e., 2 protons from -CH_2- of PVAm and 3 from CH_3 of the amine acetate). [c] Estimated based on the average molar compositions and 2,376 amino groups per PVAm molecule, estimated from its MW. [d] Estimated as d = (2,376 x 0.251)/number of carboxylic dextran 10K per molecule, where the number of amino groups per PVAm molecule is 2,376 and the length of each vinyl monomer is 0.251 nm. [e] Estimated based on assumptions of a spherical volume and a negligible PVAm and hexyl.

Table 2

	4dex$_{10k+1.5k}$-surf	**13**dex$_{10k}$-surf	dex$_{1.5k}$-surf
Single surfactant matrices			
4dex$_{10k+1.5k}$	100	-	-
13dex$_{10k}$	-	100	-
Mixed surfactant matrices			
4dex$_{10k+1.5k}$/dex$_{1.5k}$ (6:1)	75	-	25
4dex$_{10k+1.5k}$/dex$_{1.5k}$ (1:1)	50	-	50
4dex$_{10k+1.5k}$/dex$_{1.5k}$ (1:3)	25	-	75
13dex$_{10k}$/dex$_{1.5k}$ (1:1)	-	50	50

Table 3.

	Density (nmol/m^2)[a]	Separation distance between aggregates (D, nm)[b]	Reflectivity change ($\Delta\%R_{YHV}$)[c]
Non-covalently attached matrices			
4dex$_{10k+1.5k}$	181.5	62.4 ± 16.8	0.97 ± 0.22
4dex$_{10k+1.5k}$/dex$_{1.5k}$ (3:1)	172.8	73.3 ± 16.5	6.07 ± 0.22
4d ex$_{10k+1.5k}$/dex$_{1.5k}$ (1:1)	155.6	100.0 ± 30.5	7.18 ± 0.21
4dex$_{10k+1.5k}$/dex$_{1.5k}$ (1:3)	80.7	121.6 ± 37.9	4.96 ± 0.25
13dex$_{10k}$	285.1	59.3 ± 4.1	0.85 ± 0.16
13dex$_{10k}$/dex$_{1.5k}$ (1:1)	262.9	96.3 ± 10.4	3.10 ± 0.04
Covalently grafted matrix[d]	99.7	n/a	0.41± 0.04

[a]Indirectly evaluated from surface carboxylic group density determined by TBO dye assay (Xu, Persson, Löfås & Knoll, 2006) and an assumption that the allyl groups were completely converted to carboxylic acid. [b] Estimated from the height profiles of the AFM images. [c] The data are mean ± standard deviation. [d] Prepared at a concentration of 1 mg/mL.

Figure(s)

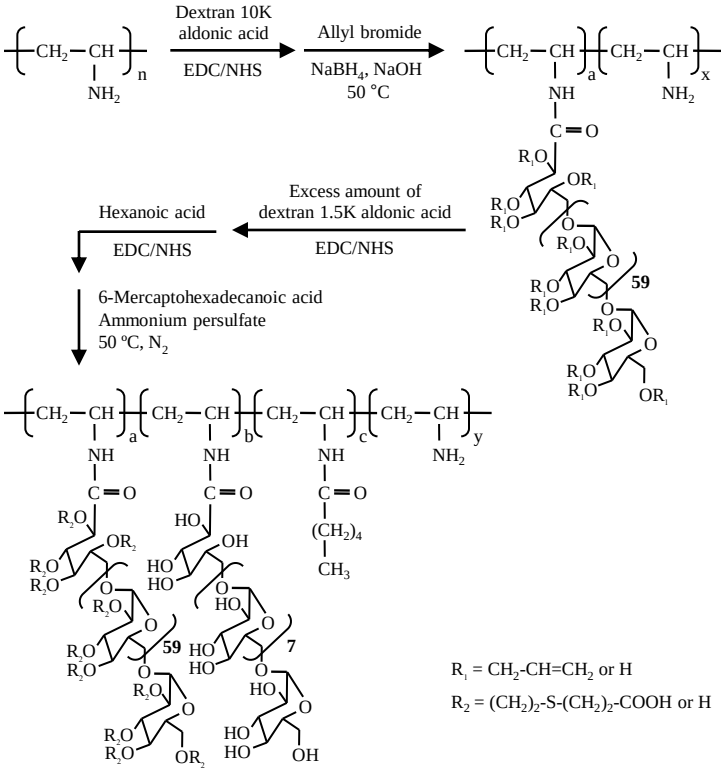

Scheme 1

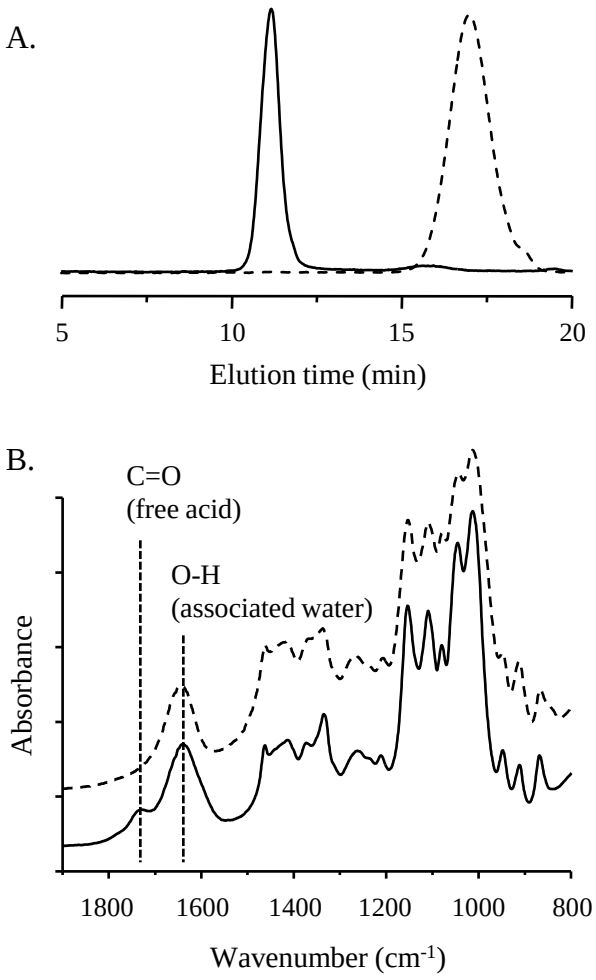
A.
5
10
15
20
Elution time (min)
B.
C=O
(free acid)
O-H
(associated water)
Absorbance
1800
1600
1400
1200
1000
800
Wavenumber (cm-1)

Figure 1

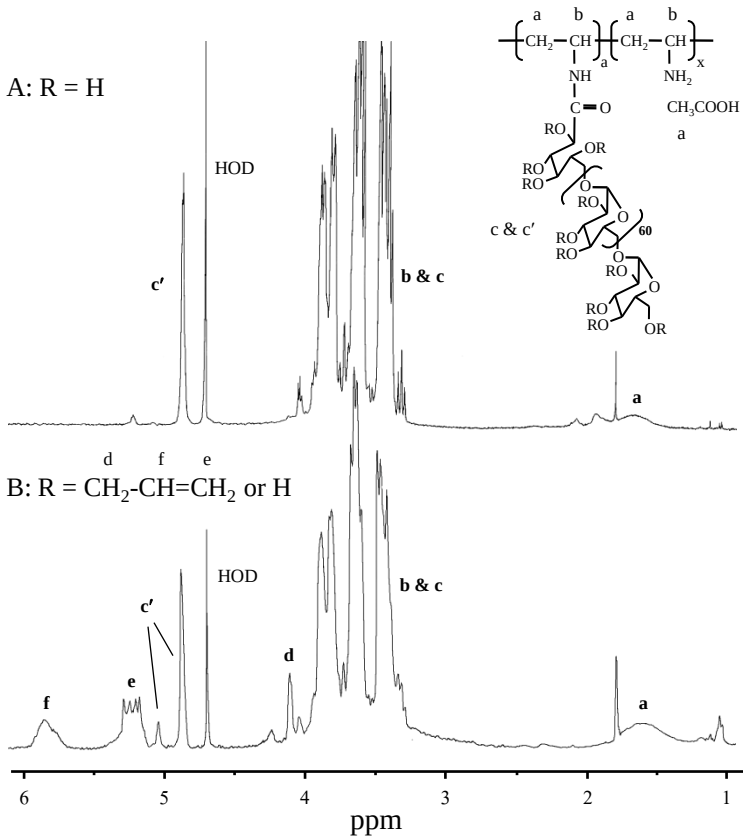
A: R = H
HOD
c′
b & c
a
d
f
e
B: R = CH2-CH=CH2 or H
HOD
b & c
c′
d
e
f
a
6
5
4
3
2
1
ppm
a
b
a
b
CH2
CH
CH2
CH
a
x
NH
NH2
C=O
CH3COOH
a
RO
OR
RO
RO
O
RO
O
60
c & c′
RO
RO
O
RO
O
RO
RO
OR

Figure 2

A.

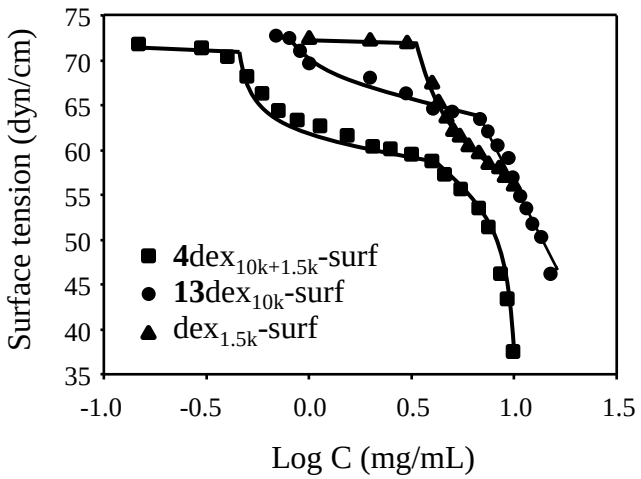
Surface tension (dyn/cm)
75
70
65
60
55
50
45
40
35
-1.0
-0.5
0.0
0.5
1.0
1.5
Log C (mg/mL)
4dex10k+1.5k-surf
13dex10k-surf
dex1.5k-surf

B.

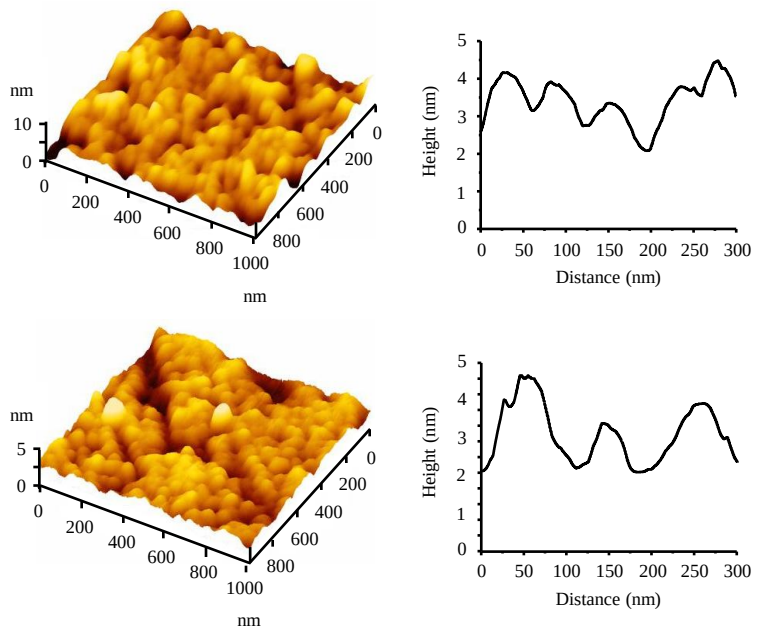
nm
10
0
0
200
400
600
800
1000
nm
Height (nm)
Distance (nm)
nm
5
0
Height (nm)
Distance (nm)

Figure 3

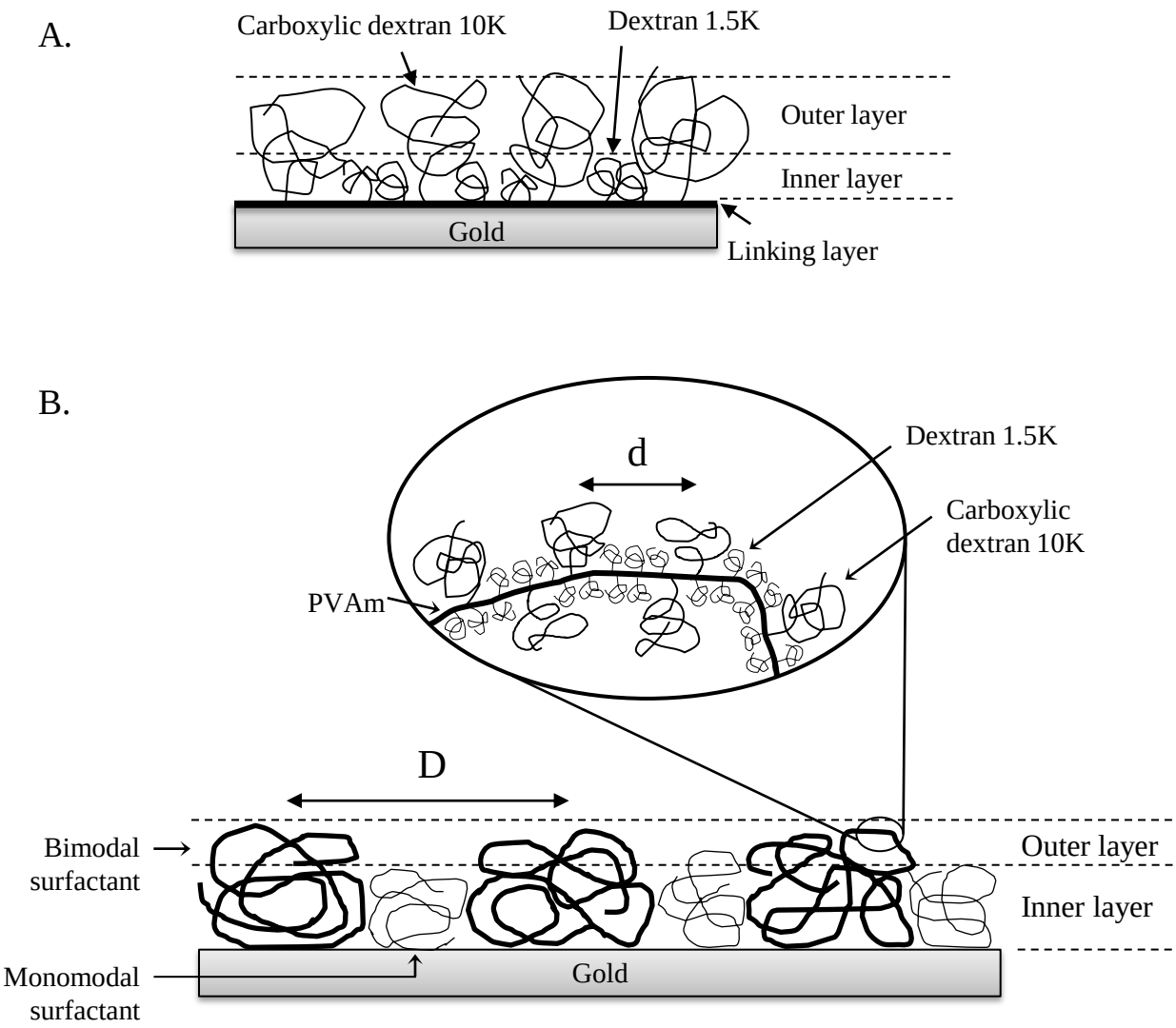
A.
Carboxylic dextran 10K
Dextran 1.5K
Outer layer
Inner layer
Gold
Linking layer
B.
d
Dextran 1.5K
Carboxylic
dextran 10K
PVAm
D
Bimodal
surfactant
Outer layer
Inner layer
Monomodal
surfactant
Gold

Figure 4

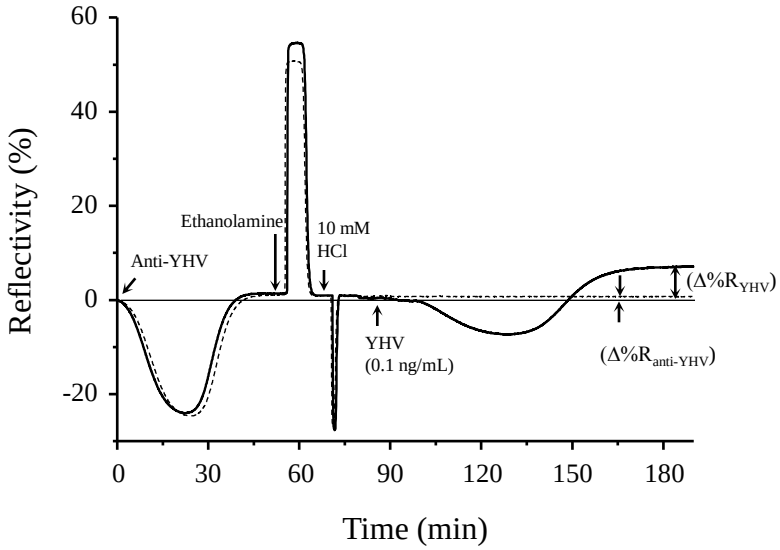
60
40
20
0
-20
Reflectivity (%)
0
30
60
90
120
150
180
Time (min)
Anti-YHV
Ethanolamine
10 mM
HCl
YHV
(0.1 ng/mL)
(Δ%R_YHV)
(Δ%R_anti-YHV)

Figure 5